Methods 183 (2020) 38–42

Contents lists available at ScienceDirect

Methods

journal homepage: www.elsevier.com/locate/ymeth

Potential functional pathways of plant RNA virus-derived small RNAs in a vector insect

Wan Zhao[a,b,1], Qiong Li[a,b,1], Feng Cui[a,b,*]

[a] State Key Laboratory of Integrated Management of Pest Insects and Rodents, Institute of Zoology, Chinese Academy of Sciences, Beijing 100101, China
[b] CAS Center for Excellence in Biotic Interactions, University of Chinese Academy of Sciences, Beijing 100049, China

ARTICLE INFO

Keywords:
Virus-derived small RNAs
Rice stripe virus
RNA virus
Argonaute proteins
RNA immunoprecipitation

ABSTRACT

During infection, RNA viruses can produce two types of virus-derived small RNAs (vsRNAs), small interfering RNA (siRNA) and microRNA (miRNA), that play a key role in RNA silencing-mediated antiviral mechanisms in various hosts by associating with different Argonaute (Ago) proteins. Ago1 has been widely identified as an essential part of the miRNA pathway, while Ago2 is required for the siRNA pathway. Thus, analysis of the interaction between vsRNAs and Ago proteins can provide a clue about which pathway the vsRNA may be involved in. In this study, using rice stripe virus (RSV)-small brown planthoppers (*Laodelphax striatellus*, Fallen) as an infection model, the interactions of eight vsRNAs derived from four viral genomic RNA fragments and Ago1 or Ago2 were detected via the RNA immunoprecipitation (RIP) method. vsRNA4-1 and vsRNA4-2 derived from RSV RNA4 were significantly enriched in Ago1-immunoprecipitated complexes, whereas vsRNA2-1 and vsRNA3-2 seemed enriched in Ago2-immunoprecipitated complexes. vsRNA1-2 and vsRNA2-2 were detected in both of the two Ago-immunoprecipitated complexes. In contrast, vsRNA1-1 and vsRNA3-1 did not accumulate in either Ago1- or Ago2-immunoprecipitated complexes, indicating that regulatory pathways other than miRNA or siRNA pathways might be employed. In addition, two conserved *L. striatellus* miRNAs were analysed via the RIP method. Both miRNAs accumulated in Ago1-immunoprecipitated complexes, which was consistent with previous studies, suggesting that our experimental system can be widely used. In conclusion, our study provides an accurate and convenient detection system to determine the potential pathway of vsRNAs, and this method may also be suitable for studying other sRNAs.

1. Introduction

Virus-derived small RNAs (vsRNAs), with 20–30 nucleotides (nt) in length, have been widely identified in various virus-infected host cells, such as plants [1], nematodes [2], arthropod [3], fungi [4], and mammals [5]. Based on the mechanisms by which they are synthesized and function, vsRNAs can be classified as microRNAs (miRNAs), small interfering RNAs (siRNAs) and piwi-interacting RNAs (piRNAs), playing key roles in RNA silencing mediated biological processes via base-pairing with their RNA targets [6]. siRNAs and miRNAs are small regulatory RNAs of 20–24 nt, processed from double-strand and stem-loop precursor RNAs respectively, by digestion with an RNase III-enzyme Dicer in either nucleus or cytoplasm [7]. In contrast, piRNAs with 26–31 nt in length, are produced in a Dicer-independent manner [8]. All of these sRNAs function as mediators in gene silencing by associating with the RNA-induced silencing complex (RISC); however, they require distinct members of the Argonaute (Ago) family [5,9]. siRNAs and miRNAs bind to the members of the Ago subclade, whereas piRNAs bind to the members of the Piwi subclade of the Ago family [10]. In many eukaryotic organisms, Ago1 has been identified as an essential component for miRNA-mediated target suppression [11–13], and has also been indicated to participate in the siRNA pathway [14,15]. The role of Ago2 has been proven to be essential for the siRNA-directed RNA interference (RNAi) response [15,16]. In fungi, such as *Neurospora crassa*, QDE2, a homolog of Ago2, has been indicated to play a role in the siRNA pathway [17]. To explore the function of new vsRNAs, they first need to be grouped in the appropriate vsRNA class. Some vsRNAs could be easily defined based on their sequence or structure characteristics. The vsiRNA pathway is directly involved in antiviral immunity in most eukaryotes, including fungi, mammals, arthropods and plants. In contrast, the production of virus-derived miRNAs appears to be more restricted[19]. However, except for rare cases, most RNA

* Corresponding author.
E-mail address: cuif@ioz.ac.cn (F. Cui).
[1] These authors contributed equally to this work.

https://doi.org/10.1016/j.ymeth.2019.10.006
Received 9 May 2019; Received in revised form 14 October 2019; Accepted 16 October 2019
Available online 22 October 2019

viruses contain an RNA genome that replicates in the cytoplasm, so it is hard to understand whether or how these virus-derived miRNAs are produced without leading to self-cleavage or destruction of the viruses' own (anti) genome [18]. Although several studies have proven that RNA viruses might encode their own miRNAs in host cells, the nucleotide structure evidence is still inadequate [20].

In this work, we used a more direct approach to explore the potential function of vsRNAs by detecting the interaction of vsRNAs and Ago1 or Ago2 via the RNA immunoprecipitation (RIP) method in rice stripe virus (RSV)-infected small brown planthopper (*Laodelphax striatellus*, Fallen). RSV is a vital rice pathogen that is efficiently transmitted by planthopper in a persistent, propagative manner [21]. RSV is an RNA virus, the genome of which contains four negative sense, single-strand RNA segments encoding seven viral proteins [22–26]. RNA1 is negative-sense, and RNA2, RNA3, and RNA4 are ambisense [23,25]. This virus has different replication and gene expression strategies in vector insect and host plant [27]. vsiRNAs induced by RSV were previously identified in the infected planthoppers, rice and tobacco [3,28]. In addition, our previous work determined the expression of vsiRNAs in RSV-infected rice and planthoppers; however, their function has not been explored [3]. In this work, we explored the potential pathway of vsRNAs by detecting the interaction of vsRNAs with Ago1 or Ago2 via the RNA immunoprecipitation (RIP) method in RSV-infected planthopper. This method was proved by us to be valid for the functional analysis of vsRNA in planthopper by detecting two conserved *L. striatellus* miRNAs. Through immunoprecipitation analysis of Ago-vsRNA complexes, we successfully detected that two vsRNAs, vsRNA4-1 and vsRNA4-2, were significantly enriched in Ago1-immunoprecipitated complexes when compared with IgG and Ago2-immunoprecipitated complexes, suggesting that these two vsRNAs might be involved in the miRNA pathway in planthoppers after infection with RSV. vsRNA2-1 and vsRNA3-2 were significantly enriched in Ago2-immunoprecipitated complexes, suggesting that they might be involved in the siRNA pathway. Our study provides a convenient method for the functional analysis of vsRNA, which could be widely used in various systems.

2. Materials

2.1. Insects

Viruliferous small brown planthoppers (*Laodelphax striatellus*, Fallen) had an RSV carrying frequency above 90% and were collected from a field population in Hai'an, Jiangsu Province, China, in 2009.

2.2. Reagents

PVDF western blotting membranes (Merck, 03010040001)

Biofuraw™ Precast Gel, 4–20% (Biofuraw, 180-8001)

PageRuler™ prestained protein ladder, 10 to 180 kDa (Thermo Fisher Scientific, 26616)

Invitrogen™ goat anti-mouse IgG (H + L) secondary antibody, HRP (Thermo Fisher Scientific, 32430)

Tween® 20 (Sigma-Aldrich, P1379)

Protein loading buffer (5x) (AdipoGen International, AG-10T-0020-L001)

Gibco™ phosphate-buffered saline (PBS buffer), pH 7.4, basic (1x) (Thermo Fisher Scientific, 10010031)

Pre-cassette gel running buffer (20x) (Biofuraw, 180-8002)

Oxoid™ skim milk powder (Thermo Fisher Scientific, LP0031B)

Mouse IgG antibody (Abcam, ab37355)

Mouse monoclonal Ago1 antibody (Beijing Protein Innovation)

Mouse monoclonal Ago2 antibody (Beijing Protein Innovation)

SuperSignal® West Femto Luminol/Enhancer Solution (Thermo Fisher Scientific, 1859022)

SuperSignal® West Femto Stable Peroxide Buffer (Thermo Fisher Scientific, 1859023)

Invitrogen™ TRIzol reagent (Thermo Fisher Scientific, 15–596-018)

Invitrogen™ Turbo DNA-free kit (Thermo Fisher Scientific, AM1907)

miRcute Plus miRNA First-Strand cDNA Kit (Tiangen, KR211) containing miRNA RT enzyme mix (50 μL), 2x miRNA RT reaction buffer (250 μL) and RNase-free ddH_2O (1 mL)

miRcute Plus miRNA qPCR Kit (SYBR Green) (Tiangen, FP411) containing 2x miRcute Plus miRNA Premix (with SYBR and ROX) (1.35 mL) and reverse primer (Tiangen, 10 μM, 55 μL)

Magna RIP™ RNA-Binding Protein Immunoprecipitation Kit (Millipore, 17–700) containing Magnetic Beads Protein A/G (CS203178, 0.66 mL), RIP wash buffer (CS203177, 2.4 mL), RIP lysis buffer (CS203176, 2.4 mL), 0.5 M EDTA (CS203175, 0.5 mL), 10% SDS (CS203174, 0.3 mL), salt solution I (CS203173, 1.0 mL), salt solution II (CS203185, 0.3 mL), protease inhibitor cocktail 200x (CS203220, 20 μL), RNase inhibitor (CS20321975, μL), proteinase K (10 mg/mL) (CS203218, 0.36 mL) and nuclease-free water (CS203217, 0.3 mL)

2.3. Equipment

Centrifuge 5424R (Eppendorf, 5424 R)

ProFlex™ 3 × 32-Well PCR System (Thermo Fisher Scientific, 4484073)

LightCycler ® 480 Real-Time PCR System (Roche, 480 II)

NanoDrop 1000 spectrophotometer (Thermo Fisher Scientific, NanoDrop 1000)

H2O3 dry bath (Coyote Bioscience, H2O3-100C)

PowerPac™ universal power supply (Bio-Rad, 1645070)

Trans-Blot® Turbo™ transfer system (Bio-Rad, 1704150)

Decolourizing shaker (YanHe, TS-200)

Tanon-5200 automatic chemiluminescence image analysis system (Tanon, Tanon-5200 Multi)

TGrinder high-speed tissue grinder (Tiangen Biotech, OSE-Y30)

Invitrogen™ MagnaRack™ magnetic separation rack (Thermo Fisher Scientific, CS15000)

2.4. Buffers

Phosphate buffer saline with Tween 20 (1x) (PBST buffer): 0.2% Tween 20 added to 1x PBS buffer, pH 7.2.

SDS-PAGE running buffer: diluted pre-cassette gel running buffer (20x) with ddH_2O for a 1x working solution.

Transfer buffer: 48 mM Tris, 39 mM glycine, 20% methanol, 0.04% SDS.

Blocking buffer: 5% skim milk added to 1 × PBST buffer.

3. Experimental design

3.1. Ago1 and Ago2 monoclonal antibody production

The amino acid sequences of the Ago1 and Ago2 antigens of the small brown planhoppers are as follows: QQPHQQPPQPPDLPMFNCPRRPNLGREGRPIVLRANHFQITMPRGFVHHYDINIQPDKCPRKVNREIIETMVTAYSKIFGNLKPVFDGRSNLYTRDPLPIGNDRMELEVTLPGEGKDRVFRVAIKWLAQVSLFALEEALEGRTRQIPYDAILALDVVMRHLPSMTYTPVGRSFFSSPDGYYHPLGGGREVWFGFHQSVRPSQWKMMLNIDVSATAFY (100-317 amino acids) for Ago1 and MGKKKGGKGRGGGASGGGDNAPSTSAPQQQRPPPQEEKPPSQPPQQLSFGAVDFPQVEHGRGGGRGGGGGDSRGRGRGRGGGRGAGGGGGESGEFQPSMTSPTEPQPSSTSTRGAWVQGRGRGRGRGGPVGDGSQRPPFQSTDTPPGFPSTPKSPPGVQQQYQQQQYQQQQYQQQPVQQQQQPVQQQQRPQPPVQQQQRPQPPFQQQQPPVQQQQQRPQPPVQQQQRPQPPVQQQQQQPPVQQQQRPQPPIQQQQRPQPSVQQQKVRS (1–268 amino acids) for Ago2. These two peptide sequences only share 4% identity, ensuring the antigen recognition specificity. Monoclonal antibodies for Ago1 and Ago2 were produced in mice (Beijing Protein Innovation). Commercial rabbit polyclonal

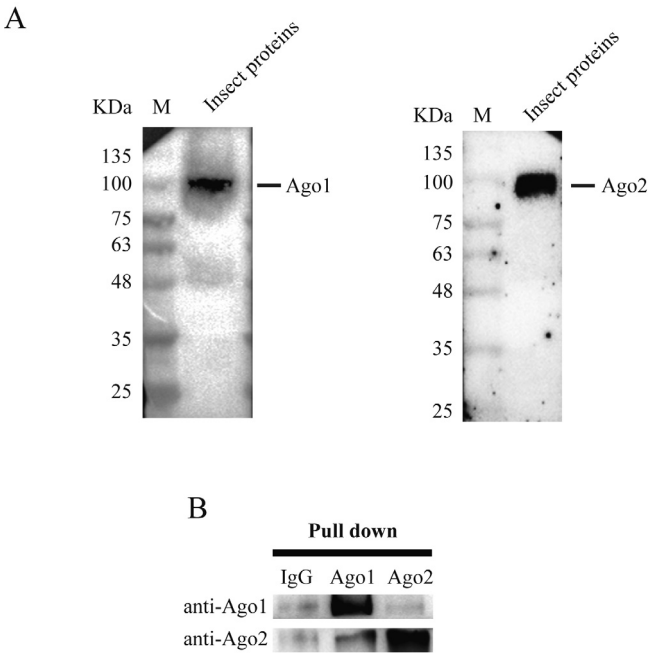

Fig. 1. Verification of Ago1 and Ago2 monoclonal antibodies by Western blotting analysis. Monoclonal antibodies for Ago1 and Ago2 were produced in mice (Beijing Protein Innovation).

antibodies to Ago1 (Abcam, ab5070) and Ago2 (Abcam, ab5072) would be applicable if the monoclonals might not be readily available.

3.2. Ago1 and Ago2 monoclonal antibody verification

Total protein was extracted from viruliferous 4th-instar small brown planthopper nymphs with PBS buffer. Proteins were subjected to Precast Gel (4–20%) electrophoresis (Biofuraw) and then transferred to PVDF membranes (Merck). Blocking was performed in 5% (wt/vol) skimmed milk at room temperature (RT) for 1 h. The PVDF membranes were incubated with primary antibody (anti-Ago1, 1:2,000; anti-Ago2, 1:2,000) in 5% (wt/vol) skimmed milk at 4 °C overnight. Goat anti-mouse IgG (H + L) secondary antibody (1:5,000) (Thermo) was incubated at RT for 1 h. Detection of the immunological blot was carried out via SuperSignal® West Femto Luminol/Enhancer Solution and Stable Peroxide Buffer (Thermo) by using Tanon-5200 automatic chemiluminescence image analysis system. A clear single target band is shown in Fig. 1, which indicates that the obtained antibodies are of high specificity and can be used for further experiments.

3.3. Immunoprecipitation of RNA-binding Protein-RNA complexes

Monoclonal antibodies against planthopper Ago1 or Ago2 protein or the mouse IgG antibody control (Abcam) were applied in the RIP assay. The experiments were performed using a Magna RIP™ RNA-Binding Protein Immunoprecipitation Kit (Merck). One biological replicate contained twenty viruliferous planthoppers.

(1) Lysate preparation

Thirty viruliferous planthoppers were homogenized in ice-cold RIP lysis buffer with a TGrinder high-speed tissue grinder (Tiangen Biotech) and stored at − 80 °C overnight for thorough tissue lysis.

(2) Magnetic bead preparation

After completely dispersing and re-suspending the magnetic beads by pipetting, 50 µL of magnetic bead suspension was transferred to each tube. Then, the magnetic beads were washed with 0.5 mL of RIP Wash Buffer three times, and the supernatant was discarded via a magnetic separator.

(3) Incubation of magnetic beads with antibodies

Five micrograms of Ago1 or Ago2 monoclonal antibody or normal mouse IgG antibody (Abcam) was incubated with magnetic beads for 30 min at RT. The supernatant was discarded, and the magnetic beads were washed with 0.5 mL of RIP Wash Buffer three times.

(4) Immunoprecipitation

The RIP Immunoprecipitation Buffer (containing 900 µL of RIP Immunoprecipitation Buffer, 35 µL of 0.5 M EDTA, 5 µL RNase inhibitor and 860 µL of RIP Wash Buffer) was prepared and co-incubated with 100 µL of the lysate supernatant and the beads-antibody complex at 4 °C overnight. Ten microliters of the supernatant of RIP lysate was prepared into a new tube as the input. After discarding the supernatant, the

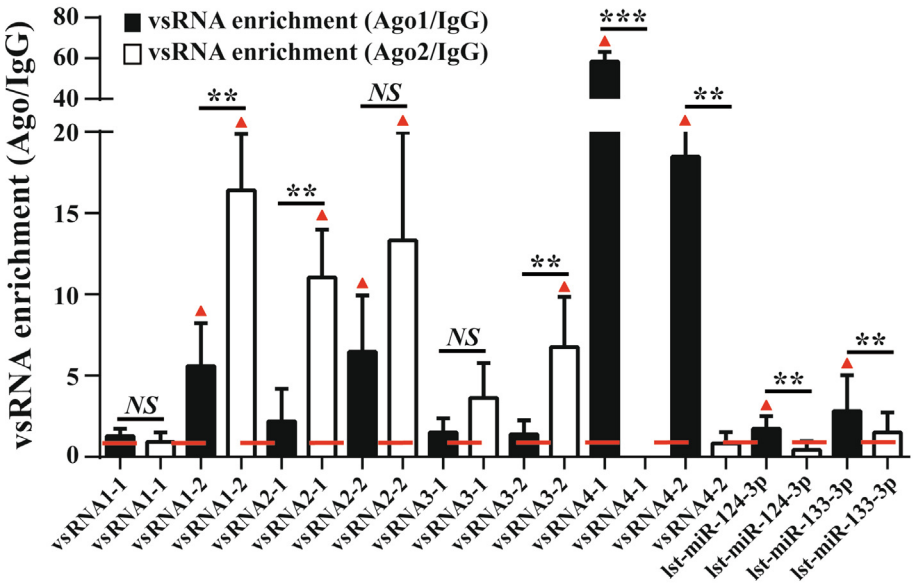

Fig. 2. Immunoprecipitation of RNA-binding Protein-RNA complexes (RIP) analysis using Ago1 and Ago2 monoclonal antibodies in viruliferous small brown planthoppers. RIP assays of the viruliferous planthoppers with antibodies against Ago1 and Ago2. The enrichment of eight vsRNAs and two conserved planthopper miRNAs was quantified by qPCR. The RNA level of each target segment relative to that of IgG control is reported as mean ± SE. A ratio of one was set as the baseline presented with a dotted red line. Values above the baseline were labelled with red triangles on top of the rectangular columns. (For interpretation of the references to colour in this figure legend, the reader is referred to the web version of this article.)

immunoprecipitate was washed with 0.5 mL of RIP Wash Buffer three times.

To demonstrate the specificity of the immunoprecipitations, 50 μL of the immunoprecipitates were applied for western blotting using Ago1 or Ago2 monoclonal antibody (Fig. 1B). In the Ago1-immunoprecipitated complexes, a strong immune signal for Ago1 was observed while a detectable signal for Ago2 was also present, indicating that the Ago1-immunoprecipitated complexes could contain a small amount of Ago2 due to the imperfect specificity of Ago1 monoclonal antibody. In Ago2-immunoprecipitated complexes, only Ago2 was detected, suggesting that the Ago2 monoclonal antibody had a high specificity. Neither Ago1 nor Ago2 was present in the IgG-immunoprecipitated complexes.

(5) Purification of RNA

The immunoprecipitate and input sample were incubated with 150 μL of proteinase K buffer (containing 117 μL of RIP Wash Buffer, 15 μL of 10% SDS and 18 μL of 10 mg/mL proteinase K) at 55 °C for 30 min with shaking for protein digestion. Next, 400 μL of phenol:-chloroform:isoamyl alcohol was added to each tube. After centrifugation at 14,000 rpm for 10 min at RT, the aqueous phase was carefully placed into a new tube. Then, 400 μL of chloroform was added. After centrifugation at 14,000 rpm for 10 min at RT, the aqueous phase was collected into a new tube. Fifty microliters of salt solution I, 15 μL of salt solution II, 5 μL of precipitate enhancer and then 850 μL of absolute ethanol were added to each tube. The mixture was kept at −80 °C for one hour to precipitate the RNA. After removal of the supernatant by centrifugation at 14,000 rpm for 30 min at 4 °C, the pellet was air dried and re-suspended in 20 μL of RNase-free water.

3.4. Reverse transcription

Each RNA sample's integrity and purity were determined using electrophoresis on 2% (w/v) agarose gel and a NanoDrop spectrophotometer (Thermo Fisher Scientific). Before cDNA synthesis, total RNA was treated using the TURBO DNA-free kit (Thermo Fisher Scientific) to remove genomic DNA contamination. One microgram of RNA was reverse transcribed to cDNA in 20 μL by using the miRNA RT enzyme Mix of miRcute Plus miRNA First-Strand cDNA Kit (Tiangen) per the manufacturer's instructions. The incubation conditions were 42 °C for 60 min, followed by 95 °C for 3 min. The miRNA RT enzyme Mix contains *E. coli* Ploy(A) polymerase, RTase and RNasin. During this process, poly(A) was added to the 3′ end of the vsRNA.

3.5. Forward primer design of vsRNA

The sRNAs of the small brown planthoppers that had acquired RSV 5 d prior were deep sequenced in our previous work and have been deposited in the Gene Expression Omnibus (GEO) database at the National Center for Biotechnology Information (NCBI) under accession number GSE113555 [3]. The sRNAs with a match to the newly obtained RSV genome [20] (and without a match to the planthopper genome) were regarded as vsiRNAs. Two vsRNAs located in the 5′ nontranslated region (NTR) or the open reading frame (ORF) of each viral RNA segment were selected for further analysis. Forward primers were designed according to the vsRNA sequences listed in Table S1. The nucleotides that marked in red were artificially added in order to obtain the optimum annealing temperature. The "GC" enrichment fragments added at the 5' ends can improve the low GC content of the original vsRNAs sequence. In addition, to establish a stronger combination with the poly (A) produced in the reverse transcription PCR, "AA" nucleotides were artificially added at the 3' ends. Each primer pair containing forward primer and the reverse primer (Tiangen) was calculated automatically by dissociation curves with a LightCycler 480 instrument (Roche). Only those primers with single dissociation peaks were considered valid primers (Fig. S1).

3.6. Relative real-time quantitative PCR

The relative expression of vsRNAs was quantified by a miRcute miRNA qPCR Detection Kit (Tiangen) with a LightCycler 480 instrument (Roche). PCRs were performed in a final volume of 10 μL, containing 1 μL of template cDNA, 5 μL of 2x miRcute Plus miRNA Premix (with SYBR and ROX) (Tiangen), and 0.25 μL of each primer (5 pmol) on the LightCycler 480® II (Roche). The thermal cycling conditions extended for 45 cycles following a standard three-step protocol of 94 °C for 20 s, followed by primer annealing/extension at 60 °C (based on the primer Tm values) for 30 s and then 72 °C for 10 s. The melting curve determination was then carried out at the end of the PCR experiment by following a three-step procedure: 94 °C for 20 s, 65 °C for 30 s and followed by stepwise temperature increase from 65 °C to 95 °C at 0.06 °C/step. The PCR products are 80–150 bp. Six to eight biological replicates were used for statistical analysis. The RNA level of each target segment relative to that of IgG control is reported as mean ± SE. A value of Ago/IgG above one indicated that the vsRNA might interact with the corresponding Ago protein. Student's *t*-test was performed to evaluate the difference between the two means using SPSS 17.0.

4. Results and discussion

As shown in Fig. 2, vsRNA4-1 and vsRNA4-2 derived from RSV RNA4 fragment were significantly enriched in Ago1-immunoprecipitated complexes compared with IgG and Ago2-immunoprecipitated complexes, demonstrating that vsRNA4-1 and vsRNA4-2 might be involved in the miRNA pathway. In contrast, vsRNA2-1 and vsRNA3-2 were only enriched in Ago2-immunoprecipitated complexes compared with IgG and Ago1-immunoprecipitated complexes, suggesting that these two vsRNAs might participate in the siRNA pathway. In addition, vsRNA1-2 and vsRNA2-2 were detected in both of the two Ago-immunoprecipitated complexes. Considering that the Ago1-immunoprecipitated complexes could contain a small amount of Ago2 due to the imperfect specificity of Ago1 monoclonal antibody (Fig. 1B), vsRNA1-2 and vsRNA2-2 could mainly reside in Ago2-immunoprecipitated complexes and participate in the siRNA pathway. Different from other vsRNAs, vsRNA1-1 and vsRNA3-1 did not accumulate in either Ago1- or Ago2-immunoprecipitated complexes, suggesting that a different regulatory pathway might be involved.

In addition, to verify whether this experimental system is applicable to other sRNAs, two conserved miRNAs, lst-miR-124-3p and lst-miR-133-3p[26], identified in planthoppers, were also analysed via RIP experiments. As shown in Fig. 2, both were significantly enriched in Ago1-immunoprecipitated complexes, which was consistent with previous research. In conclusion, our study provided an accurate and convenient detection system to determine the potential pathway of vsRNAs and classical sRNAs.

5. Conclusions

We explored the potential pathways of vsRNAs by detecting the interaction of eight vsRNAs with Ago1 or Ago2 in vector insects via the RIP method. These viral small RNAs may utilize both miRNA and siRNA pathway for functioning in vector insects. This method is valid for the functional study of viral small RNAs in the system of RSV and its vector insect.

Acknowledgements

This work was funded by the grant of the Chinese Academy of Sciences (No. ZDBS-LY-SM027), the Major Special Projects for Infectious Diseases during the 13th 5-year plan of China (No.

2017ZX10303404) and the National Key R&D Program of China (No. 2017YFD0200400).

Appendix A. Supplementary data

Supplementary data to this article can be found online at https://doi.org/10.1016/j.ymeth.2019.10.006.

References:

[1] Y. Zhang, B.E. Wiggins, C. Lawrence, J. Petrick, S. Ivashuta, G. Heck, Analysis of plant-derived miRNAs in animal small RNA datasets, BMC Genom. 13 (2012) 381–381.

[2] X. Guo, W.-X. Li, R. Lu, Silencing of host genes directed by virus-derived short interfering RNAs in *Caenorhabditis elegans*, J. Virol. 86 (21) (2012) 11645–11653.

[3] M. Yang, Z. Xu, W. Zhao, Q. Liu, Q. Li, L. Lu, R. Liu, X. Zhang, F. Cui, Rice stripe virus-derived siRNAs play different regulatory roles in rice and in the insect vector Laodelphax striatellus, BMC Plant Biol. 18 (1) (2018) 219.

[4] S.-Y. Lee Marzano, A. Neupane, L. Domier, Transcriptional and small RNA responses of the white mold fungus sclerotinia sclerotiorum to infection by a virulence-attenuating hypovirus, Viruses 10 (12) (2018) 713.

[5] K.F. Weng, P.T. Hsieh, H.I. Huang, S.R. Shih, Mammalian RNA virus-derived small RNA: biogenesis and functional activity, Microb. Infect. 17 (8) (2015) 557–563.

[6] M.L. Li, K.F. Weng, S.R. Shih, G. Brewer, The evolving world of small RNAs from RNA viruses, Wiley Interdiscip. Rev. RNA 7 (5) (2016) 575–588.

[7] R.W. Carthew, E.J. Sontheimer, Origins and Mechanisms of miRNAs and siRNAs, Cell 136 (4) (2009) 642–655.

[8] C. Kutter, P. Svoboda, miRNA, siRNA, piRNA: Knowns of the unknown, RNA Biol. 5 (4) (2008) 181–188.

[9] S.M. Hammond, E. Bernstein, D. Beach, G.J. Hannon, An RNA-directed nuclease mediates post-transcriptional gene silencing in Drosophila cells, Nature 404 (6775) (2000) 293–296.

[10] N. Matsumoto, H. Nishimasu, K. Sakakibara, K.M. Nishida, T. Hirano, R. Ishitani, H. Siomi, M.C. Siomi, O. Nureki, Crystal Structure of Silkworm PIWI-Clade Argonaute Siwi Bound to piRNA, Cell 167 (2) (2016) 484–497.e9.

[11] S. Asgari, Role of MicroRNAs in insect host-microorganism interactions, Front. Physiol. 2 (2011) 48–48.

[12] J. He, Q. Chen, Y. Wei, F. Jiang, M. Yang, S. Hao, X. Guo, D. Chen, L. Kang, MicroRNA-276 promotes egg-hatching synchrony by up-regulating *brm* in locusts, Proceed. Natl. Acad. Sci. 113 (3) (2016) 584–589.

[13] G. Ren, M. Xie, S. Zhang, C. Vinovskis, X. Chen, B. Yu, Methylation protects microRNAs from an AGO1-associated activity that uridylates 5' RNA fragments generated by AGO1 cleavage, Proceed. Natl. Acad Sci. U.S.A. 111 (17) (2014) 6365–6370.

[14] A.E. Martínez de Alba, V. Jauvion, A.C. Mallory, N. Bouteiller, H. Vaucheret, The miRNA pathway limits AGO1 availability during siRNA-mediated PTGS defense against exogenous RNA, Nucl. Acid Res. 39 (21) (2011) 9339–9344.

[15] K. Fátyol, M. Ludman, J. Burgyán, Functional dissection of a plant Argonaute, Nucl. Acid. Res. 44 (3) (2016) 1384–1397.

[16] V. Bhandare, A. Ramaswamy, Structural dynamics of human argonaute2 and its interaction with siRNAs designed to target mutant tdp43, Adv. Bioinform. 2016 (2016) 8792814-8792814.

[17] C. Catalanotto, G. Azzalin, G. Macino, C. Cogoni, Involvement of small RNAs and role of the qde genes in the gene silencing pathway in Neurospora, Gen. Dev. 16 (7) (2002) 790–795.

[18] L.C. Aguado, B. tenOever, RNA virus building blocks-miRNAs not included, PLoS Pathog. 14 (5) (2018) e1006963.

[19] S. Pfeffer, M. Zavolan, F.A. Grässer, M. Chien, J.J. Russo, J. Ju, B. John, A.J. Enright, D. Marks, C. Sander, T. Tuschl, Identification of virus-encoded microRNAs, Science 304 (5671) (2004) 734–736.

[20] G. Swaminathan, J. Martin-Garcia, S. Navas-Martin, RNA viruses and microRNAs: challenging discoveries for the 21st century, Physiol. Genom. 45 (22) (2013) 1035–1048.

[21] W. Zhao, P. Yang, L. Kang, F. Cui, Different pathogenicities of Rice stripe virus from the insect vector and from viruliferous plants, New Phytol. 210 (1) (2016) 196–207.

[22] W. Zhao, Z. Xu, X. Zhang, M. Yang, L. Kang, R. Liu, F. Cui, Genomic variations in the 3'-termini of rice stripe virus in the rotation between vector insect and host plant, New Phytol. 219 (3) (2018) 1085–1096.

[23] Y. Zhu, T. Hayakawa, S. Toriyama, M. Takahashi, Complete nucleotide sequence of RNA 3 of rice stripe virus: an ambisense coding strategy, J. Gen. Virol. 72 (4) (1991) 763–767.

[24] S. Toriyama, An RNA-dependent RNA polymerase associated with the filamentous nucleoproteins of rice stripe virus, J. Gen. Virol. 67 (1986) 9.

[25] C. Hamamatsu, S. Toryama, T. Toyoda, A. Ishihama, Ambisense coding strategy of the rice stripe virus genome: in vitro translation studies, J. Gen. Virol. 74 (1993) 7.

[26] P. Chomchan, G.J. Miranda, Y. Shirako, Detection of rice grassy stunt tenuivirus nonstructural proteins p2, p5 and p6 from infected rice plants and from viruliferous brown planthoppers, Arch. Virol. 147 (12) (2002) 2291–2300.

[27] W. Zhao, Q. Wang, Z. Xu, R. Liu, F. Cui, Distinct replication and gene expression strategies of the Rice stripe virus in vector insects and host plants, J. Gen. Virol. 100 (5) (2019) 877–888.

[28] F. Yan, H. Zhang, M.J. Adams, J. Yang, J. Peng, J.F. Antoniw, Y. Zhou, J. Chen, Characterization of siRNAs derived from rice stripe virus in infected rice plants by deep sequencing, Arch. Virol. 155 (6) (2010) 935–940.